ACS Macro Letters

pubs.acs.org/macroletters Letter

Effect of Dispersity on the Conformation of Spherical Polymer Brushes

Tzu-Han Li, Vivek Yadav, Jacinta C. Conrad,* and Megan L. Robertson*

Cite This: ACS Macro Lett. 2021, 10, 518−524 Read Online

ACCESS | Metrics & More | Article Recommendations | Supporting Information

ABSTRACT: We show that dispersity ($Đ$) markedly alters the conformation of spherical polymer brushes. The average lengths (l_b) of poly(*tert*-butyl acrylate) (P*t*BA) brushes of varying $Đ$ grafted to nanoparticles were measured using dynamic light scattering. In the semidilute polymer brush (SDPB) regime, the l_b of P*t*BA and polymers from earlier studies of various $Đ$ could be cleanly collapsed onto a master curve as a function of the scaling variable $N_w\sigma^{1/3}$, where N_w is the weight-average degree of polymerization and σ is the grafting density. In the concentrated polymer brush (CPB) regime, however, l_b collapsed onto a bifurcated curve as a function of the scaling variable $N_w\sigma^{1/2}$, indicating $Đ$ more strongly affects the average length of brushes with low $N_w\sigma^{1/2}$. We propose that the stretching of the stem near the particle surface due to interchain interactions in the CPB regime leads to greater l_b in broad dispersity brushes of low but not high $N_w\sigma^{1/2}$.

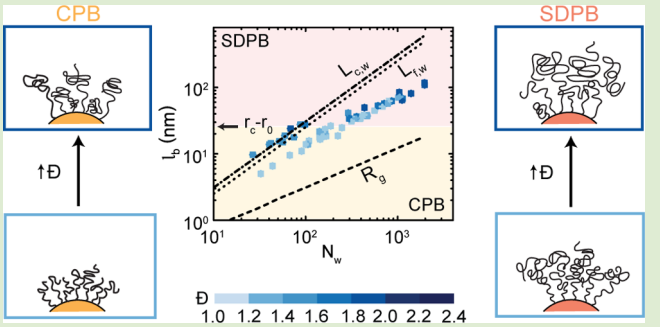

Polymer-grafted nanoparticles (PGNPs) have been widely applied as mechanical reinforcement fillers[1−3] and in optics and electronics,[4−6] ultrafiltration membranes,[7,8] biomolecular and drug delivery vehicles,[9−11] and lubrication.[12−14] The functional properties of PGNPs are determined in part through the conformation of the grafted polymer chains, which can be modified through control over the brush parameters. Indeed, the degree of polymerization (N), grafting density (σ), and dispersity ($Đ$), related to the breadth of the molecular weight distribution, of the polymer brushes can be tailored using controlled polymerizations.[15−25] Despite advances in control over surface-grafted polymer brushes, the effects of the brush molecular weight distribution on conformation remain incompletely understood.

The conformation of polymer brushes is commonly predicted using a scaling theory, in which the average brush length (l_b) scales with σ and N.[26−34] In theories for spherical brushes in a good solvent, interactions between monomers at low σ are treated as pairwise and the brush is assumed to be in the semidilute polymer brush (SDPB) regime. In the SDPB regime, l_b is predicted to scale as[26,35]

$$l_b \sim (N\sigma^{1/3})^{3/5} \quad (1)$$

With sufficiently high σ, polymer chains in a good solvent experience higher-order segmental interactions and excluded-volume effects are screened. For brushes in this concentrated polymer brush (CPB) regime, the scaling behavior becomes[26,35]

$$l_b \sim (N\sigma^{1/2})^x \quad (2)$$

where $3/5 < x \leq 1$. To account for a decrease in brush density with increasing distance from the nanoparticle surface, the conformation of spherical brushes is assumed to transition from CPB to SDPB at a critical radius r_c.[26,35]

It is not immediately evident, however, how to incorporate changes in brush conformation arising in a brush of even modest $Đ$. To address this gap, the conformation of high-$Đ$ brushes was examined using theory and simulations.[36,37] In a higher dispersity brush, short chains were collapsed toward the surface; long chains adopted a stretched stem conformation near the surface when surrounded by smaller chains but collapsed at the periphery in the crown region.[36,37] Although many experimental studies report brush $Đ$, relatively few have examined its effect on brush conformation. A recent experimental study examining the conformation of polycaprolactone (PCL) brushes with $Đ$ = 1.42−2.39 showed that average brush thickness increased with increasing $Đ$ and σ.[38] The scaling exponents of l_b with N, however, were markedly greater than unity, the upper limit of the scaling theory in the CPB regime.[26] Differences in l_b in brushes of varying $Đ$, and therefore the scaling exponents, were hypothesized to arise from differences in hydrodynamic interactions and brush

Received: January 11, 2021
Accepted: April 5, 2021

https://doi.org/10.1021/acsmacrolett.0c00898
ACS Macro Lett. 2021, 10, 518−524

conformation. Nonetheless, how these observations connect to predictions of scaling theory is not clear.

In this Letter, we show that the effect of polymer $Đ$ on the conformation of spherical polymer brushes depends strikingly on brush molecular weight. We synthesized poly(*tert*-butyl acrylate) (P*t*BA) brushes of $Đ$ = 1.03−1.98 grafted to nanoparticles using surface-initiated-atom-transfer radical polymerization (SI-ATRP) and determined l_b using dynamic light scattering (DLS) in a good solvent. The average lengths of brushes exceeded the number-average contour length ($L_{c,n}$) predicted from the number-average degree of polymerization (N_n), indicating that long chains contributed significantly to the measured l_b. In the SDPB regime, l_b of brushes of various $Đ$ could be collapsed onto a master curve as a function of the scaling variable $N_w\sigma^{1/3}$, where N_w is the weight-average degree of polymerization. In the CPB regime, however, l_b collapsed onto a bifurcated curve as a function of the scaling variable $N_w\sigma^{1/2}$, revealing that $Đ$ more strongly affects the average lengths of brushes of low $N_w\sigma^{1/2}$. Polymer brushes of various $Đ$ from the literature also collapsed onto these curves.[26,35,38,39] To explain the bifurcation in the CPB regime, we propose that stretching of the stem region in disperse brushes leads to an increase in average l_b only when $N_w\sigma^{1/2}$ is low.

P*t*BA brushes were grown from silica nanoparticles with an average core radius (r_0) of 5.7 ± 0.2 nm as measured by DLS via SI-ATRP,[25,38] and brush $Đ$ was tuned between 1.03 and 1.98 with the addition of phenylhydrazine to selected syntheses.[15] Grafted polymer was cleaved from nanoparticles using aqueous hydrofluoric acid (Sigma-Aldrich, 49%) for molecular weight and $Đ$ characterization via gel permeation chromatography (GPC). σ = 0.5 ± 0.2 chains/nm^2 was calculated from the weight percentage of grafted polymer, determined using thermogravimetric analysis (TGA) and elemental analysis (EA) (σ of individual samples are listed in the Supporting Information). From the hydrodynamic radius (R_h) of the PGNPs, characterized via the method of cumulants applied to DLS data, we calculated $l_b = R_h - r_0$ (Supporting Information).[40]

Increasing the brush $Đ$ had different consequences for l_b, depending on N_w. At $N_w \approx 43$, the characteristic time scale extracted from the intensity−intensity correlation functions increased with $Đ$ (Figure 1a), indicating that R_h of the PGNP and hence l_b were greater. At higher $N_w \approx 833$, however, the intensity−intensity correlation functions obtained for brushes of two different $Đ$ were identical (Figure 1b), indicating that R_h did not change with an increase in $Đ$. This surprising result suggests that $Đ$ markedly alters l_b only in a range of N_w.

Prior studies on brush conformation examined l_b scaling behavior with both N_n [1,25,36,38,39,41,42] and N_w,[2,26,35,43] without clear consensus as to which molecular weight-average governs brush behavior. To assess the effects of $Đ$ on l_b, we first examined l_b as a function of N_n. When $Đ$ was increased from low (1.03−1.29) to high (1.49−1.98), l_b increased at constant N_n, reflecting contributions from long chains in the broad molecular weight distribution (Figure 2a). At lower values of N_n, l_b of high-$Đ$ brushes was greater than the number-average contour length determined as the full length of a P*t*BA chain adopting a linear conformation ($L_{c,n} = N_n l_0$) and the number-average fully extended length determined as the length of the all-*trans* conformation ($L_{f,n} = N_n l_0 \sin\frac{\theta}{2}$), where l_0 = 0.30 nm (the length of 2 carbon−carbon bonds) and θ = 109.5° were the monomer length and carbon−carbon bond angle,

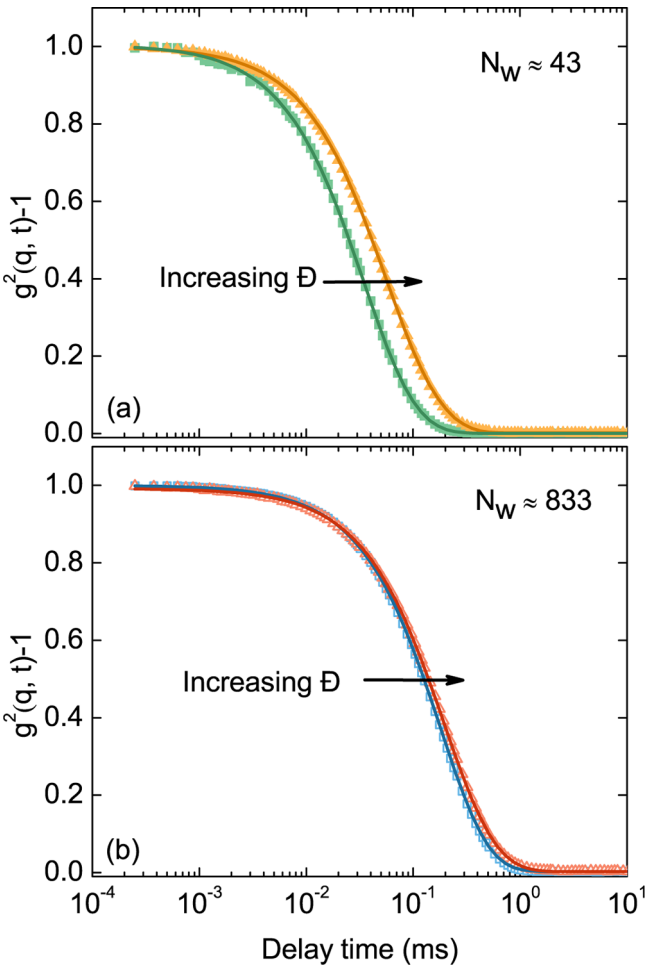

Figure 1. Intensity−intensity correlation functions $g^2(q,t) - 1$ as a function of delay time for PGNPs with a similar weight-average degree of polymerization N_w and varying $Đ$ were collected in a good solvent, THF, with concentration 1 mg mL^{-1} at 20 °C. Solid lines represent the method of cumulant fits.[40] (a) N_w = 45, $Đ$ = 1.05 (green closed squares), N_w = 41, $Đ$ = 1.50 (yellow closed triangles); (b) N_w = 802, $Đ$ = 1.23 (blue open squares), N_w = 864, $Đ$ = 1.69 (red open triangles).

respectively (Supporting Information).[44−46] This intriguing result confirms that long chains contribute substantially to l_b when the molecular weight distribution is broad. All l_b were greater than the radius of gyration ($R_g = 1.18 \times 10^{-2} M^{0.59}$, obtained from free P*t*BA in THF,[47] where M was the number-average and weight-average molecular weight in Figure 2a,b, respectively), consistent with prior literature, demonstrating R_g of grafted chains was greater than that of free chains at high grafting density.[48]

To account for long chains in a broad molecular weight distribution, we compared the dependence of l_b on N_w with the weight-average contour length ($L_{c,w} = N_w l_0$) and the weight-average fully extended length ($L_{f,w} = N_w l_0 \sin\frac{\theta}{2}$).[44−46] The l_b values of the high-$Đ$ series were commensurate with $L_{c,w}$ and $L_{f,w}$ when $N_w \leq 100$, and the l_b of the other brushes were between $L_{c,w}$ and R_g, regardless of $Đ$ and N_w (Figure 2b). To locate the crossover from CPB to SDPB brush regimes, r_c was calculated as[2,38,49]

$$r_c = r_0(\sigma^*)^{0.5}(\upsilon^*)^{-1} \quad (3)$$

https://doi.org/10.1021/acsmacrolett.0c00898
ACS Macro Lett. 2021, 10, 518−524

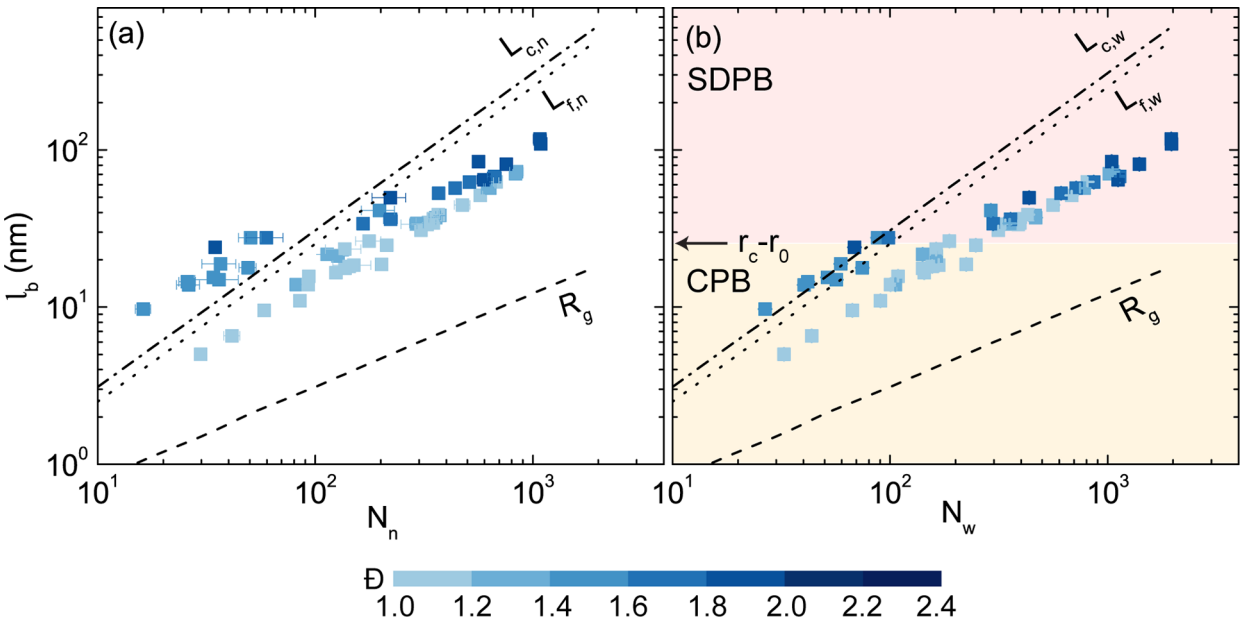

Figure 2. Average brush length l_b as a function of (a) N_n and (b) N_w. The dashed-dotted lines indicate $L_{c,n}$ in part a and $L_{c,w}$ in part b. The dotted lines indicate $L_{f,n}$ in part a and $L_{f,w}$ in part b. The dashed lines indicate R_g. The boundary between the CPB and the SDPB regimes was determined as $l_b = r_c - r_0 = 26 \pm 5$ nm using eq 3. The symbol's color shading indicates brush $Đ$. Error bars, smaller than the symbols if not visible, were determined from multiple measurements using DLS (l_b) or GPC (N_n and N_w).

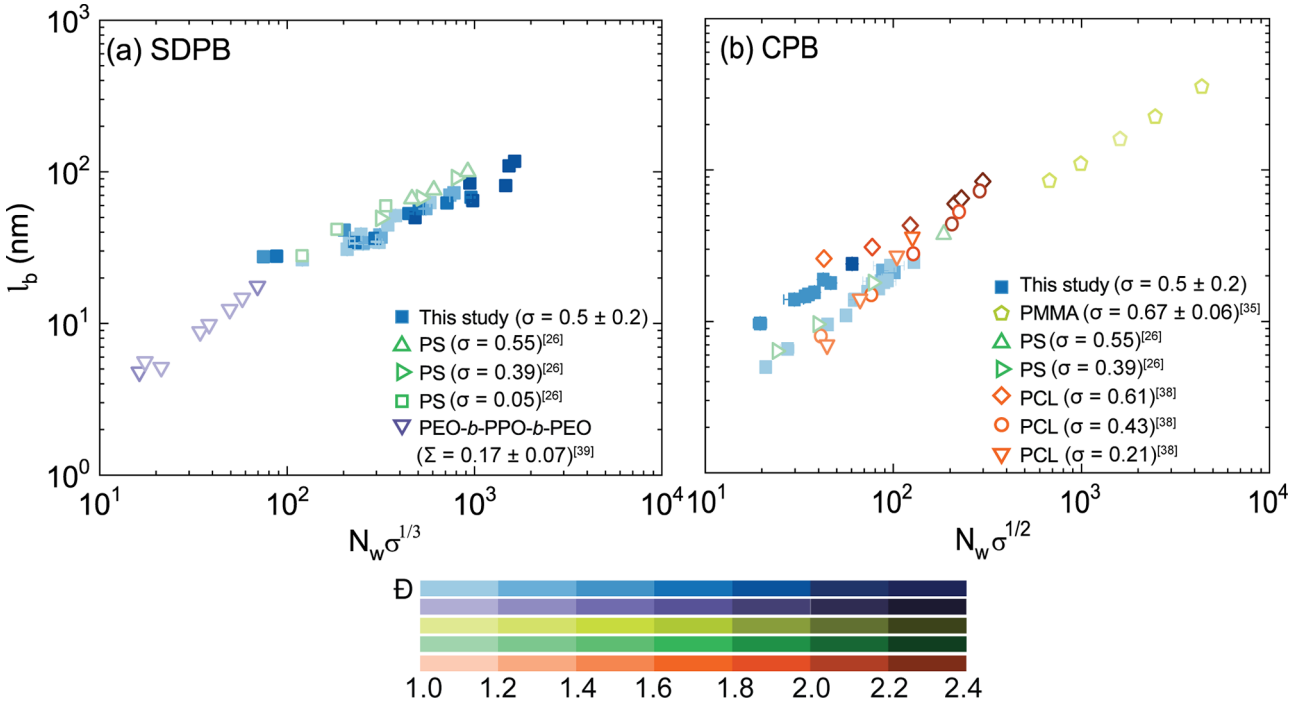

Figure 3. l_b as a function of (a) $N_w\sigma^{1/3}$ in the SDPB regime and (b) $N_w\sigma^{1/2}$ in the CPB regime, in which the color shading indicates $Đ$. The blue series represents the P*t*BA-grafted silica nanoparticles in this study ($Đ$ = 1.03−1.98, σ = 0.5 ± 0.2 chains/nm^2). The green series represents PS-grafted silica nanoparticles ($Đ$ = 1.05−1.13, σ = 0.05−0.55 chains/nm^2).[26] The yellow series represents PMMA-grafted silica nanoparticles ($Đ$ = 1.19−1.28, σ = 0.59−0.73 chains/nm^2).[35] The purple series represents PEO-*b*-PPO-*b*-PEO adsorbed triblock copolymer silica nanoparticles ($Đ$ = 1.10−1.20, brush adsorbed amount Σ = 0.11−0.30 chains/nm^2).[39] The orange series represents PCL-grafted silica nanoparticles ($Đ$ = 1.42−2.39, σ = 0.21−0.61 chains/nm^2).[38]

where $\sigma^* = \sigma b^2$ was the reduced grafting density, υ was the excluded volume parameter, and $\upsilon^* = \upsilon/(4\pi)^{1/2}$. Equation 3 was previously applied to brushes grafted from nanoparticles with r_0 varying from 5 to 65 nm.[26,35,38,50,51] For P*t*BA brushes, r_c = 32 ± 5 nm using eq 3 (b = 0.7 nm,[52,53] and υ = 0.23 ± 0.06, calculated using the MWC-WZ model [Supporting Information]).[26] Thus, brushes with l_b < 26 nm were in the CPB regime, where the l_b of high-$Đ$ brushes was greater than that of low-$Đ$ brushes. Brushes with l_b > 26 nm were in the SDPB regime, and l_b collapsed onto a master curve regardless of $Đ$.

https://doi.org/10.1021/acsmacrolett.0c00898
ACS Macro Lett. 2021, 10, 518−524

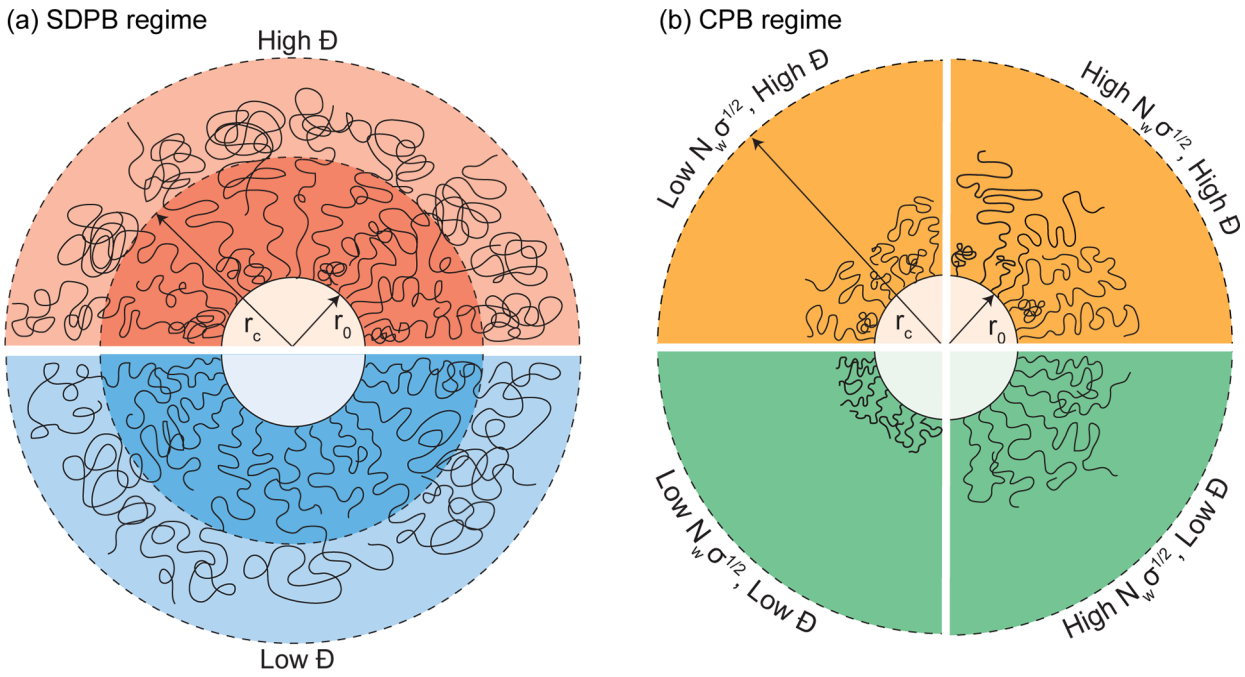

Figure 4. Schematic representation of the conformation of polymer-grafted nanoparticles with core radius r_0 in different regimes. (a) Low-Đ and high-Đ brushes above a critical radius r_c are in the SDPB regime at the periphery with similar l_b and coiled conformation. (b) Brushes below r_c are in the CPB regime with varying Đ and $N_w\sigma^{1/2}$. At low $N_w\sigma^{1/2}$, the stem of long chains at high Đ is more extended than that at low Đ. At high $N_w\sigma^{1/2}$, the differences in l_b and conformation at the periphery of brushes with low and high Đ are less distinguishable.

Next, we examined l_b of brushes in the SDPB and CPB regimes as a function of $N_w\sigma^{1/3}$ and $N_w\sigma^{1/2}$, respectively.[26] The use of scaling theory allows us to compare multiple brush systems at different σ.[26] In the SDPB regime, l_b of P*t*BA brushes (Đ = 1.03−1.96) as well as brushes composed of polystyrene (PS, Đ = 1.05−1.13)[26] and a poly(ethylene oxide-*block*-propylene oxide-*block*-ethylene oxide) triblock copolymer (PEO-*b*-PPO-*b*-PEO, Đ = 1.10−1.20)[39] collapsed cleanly onto a master curve as a function of $N_w\sigma^{1/3}$ (Figure 3a), independent of Đ. Thus, Đ does not markedly alter l_b in the SDPB regime.

In the CPB regime, however, short brushes of low-Đ (PS, PMMA, PCL, and P*t*BA) and high-Đ (PCL and P*t*BA) scaled onto a bifurcated curve as a function of $N_w\sigma^{1/2}$ (Figure 3b). The l_b values of brushes of varying compositions and dispersities fell on two distinct curves that intersected at $N_w\sigma^{1/2}$ = 470 ± 30 (Figure S5). High-Đ P*t*BA brushes (Đ = 1.49−1.98) collapsed onto the high-Đ branch along with the high-Đ PCL brushes (Đ = 1.69−2.39).[38] Low-Đ P*t*BA brushes (Đ = 1.03−1.29) collapsed onto the low-Đ branch with PS (Đ = 1.06 and 1.08)[26] and PMMA brushes (Đ = 1.19−1.28).[35] Interestingly, PCL brushes with moderate Đ (Đ = 1.42−2.06) also collapsed on this branch (Figure 3b).[38] This result suggests that the σ-dependence of the scaling of higher-Đ brushes may not follow that of uniform brushes. This idea, to be discussed later, is consistent with earlier Monte Carlo (MC) simulations, which revealed that l_b of brushes with Đ = 1.5−2.5 scaled as $l_b \sim \sigma^{0.113\pm0.009}$.[36] Nonetheless, for each polymer composition, l_b in the high-Đ branch was greater than that in the low-Đ branch for $N_w\sigma^{1/2} < 470 \pm 30$; by contrast, l_b collapsed onto one curve at higher $N_w\sigma^{1/2}$ independent of Đ (Figure 3b).

Through a linear fit to P*t*BA brush data (Figure S6), we extracted the scaling exponents (eqs 1 and 2). These exponents were 0.55 ± 0.03 in the SDPB regime and 0.9 ± 0.1 and 0.82 ± 0.07 for low-Đ and high-Đ branches, respectively, in the CPB regime, consistent with scaling theory. PCL brushes exhibited a similar trend in scaling exponent to P*t*BA brushes in the CPB regime: the exponent of the low-Đ branch was higher than that of the high-Đ branch, though the exponent of the low-Đ branch exceeded 1.[38] Though the scaling theory was developed for low-Đ brushes, literature studies on high-Đ planar brushes confirmed their scaling exponents for N and σ were consistent with that of low-Đ brushes.[37]

The independence of l_b with varying Đ in the SDPB regime suggests that all brushes adopt a similar coiled conformation. In the CPB regime, however, at low $N_w\sigma^{1/2}$, higher-Đ brushes adopt a more extended conformation than lower-Đ brushes, whereas the brush conformation at the periphery is independent of Đ at higher $N_w\sigma^{1/2}$. To explain these contrasting effects of Đ, we propose physical pictures for brushes in the two regimes. The hypothesized conformation of brushes in the SDPB regime with varying Đ is depicted in Figure 4a. At high l_b, the brush transitions from the CPB regime to the SDPB regime when l_b exceeds r_c, such that polymer chains adopt a coiled conformation at the periphery.[26,35] We propose that the coiled morphology at the periphery is not strongly influenced by Đ (Figure 4a). Thus, the average l_b is relatively insensitive to Đ in the SDPB regime.

The proposed conformation of brushes in the CPB regime with varying $N_w\sigma^{1/2}$ and Đ is depicted in Figure 4b. In the CPB regime, polymer chains in close proximity experience higher-order interactions.[26,35] For high-Đ brushes, based on earlier theories and simulations, we suggest that steric hindrance due to compressed short chains near the surface drives the extension of longer chains.[36,37] The long chains extend near the particle surface (the "stem") in the vicinity of shorter chains but are less stretched at their free ends (the "crown").[36,37] It is this highly extended stem that leads to the experimental observation of greater l_b for the high-Đ

https://doi.org/10.1021/acsmacrolett.0c00898
ACS Macro Lett. 2021, 10, 518−524

brushes compared to the low-$Đ$ brushes at low $N_w\sigma^{1/2}$. At higher $N_w\sigma^{1/2}$, however, we suggest that the conformation at the periphery is not strongly affected by $Đ$, and hence, the difference in l_b between high-$Đ$ and low-$Đ$ brushes is negligible.

This picture is consistent with earlier MC simulations, which found that the effect of $Đ$ on monomer density varied with σ.[36] At constant N_n, when σ = 0.65 and 0.25 chains/b^2, the monomer density at intermediate distance from the grafted surface decreased with increasing $Đ$, indicating that the chains were extended near the surface.[36] When σ decreased from 0.25 to 0.1 chains/b^2, however, this monomer density became less dependent on $Đ$.[36] The nearly identical monomer density profiles of brushes of various $Đ$ at the lowest σ suggests that these brushes do not adopt a stem configuration near the surface. This comparison suggests that the demarcation between high- and low-$Đ$ regimes is affected by σ. To test this idea, we compare σ (chains/b^2) of the PCL brushes in Figure 3b (for which moderate-$Đ$ brushes collapsed onto the low-$Đ$ branch) with that of the MC simulations (Table S1). For PCL brushes, a grafting density of σ = 0.21 chains/nm^2 corresponded to σ = 0.08 chains/b^2, at which the effect of $Đ$ on PCL brush conformation was negligible in simulations.[36] Indeed, PCL brushes with σ = 0.21 chains/nm^2 adopted a similar conformation as that for low-$Đ$ brushes, explaining the collapse of l_b for these brushes onto the low-$Đ$ branch (Figure 3b). Likewise, the grafting density of moderate-$Đ$ PCL brushes, σ = 0.43 chains/nm^2 (σ = 0.15 chains/b^2), was less than the σ = 0.25 chains/b^2 at which stems were observed in simulations. We conclude that l_b of high-$Đ$ brushes is controlled by the extended stem region, which is not present at low σ.

In conclusion, we investigated the dependence of l_b of polymer brushes grafted to nanoparticles on $Đ$. The transition from the CPB to the SDPB regimes was independent of brush $Đ$, and l_b of P*t*BA brushes collapsed in the SDPB regime but fell on a bifurcated curve in the CPB regime. Significantly, l_b of brushes of various polymers (from literature studies) also collapsed onto the same master curve in the SDPB regime and onto the same bifurcated curve in the CPB regime. We therefore propose that the coiled conformation is independent of $Đ$ in the SDPB regime. In the CPB regime, the high-$Đ$ brushes adopted a more extended conformation than the low-$Đ$ brushes when $N_w\sigma^{1/2} < 470 \pm 30$, yet brushes of differing $Đ$ adopted a similar conformation at the periphery at higher $N_w\sigma^{1/2}$. The more extended polymer brush conformation attained via an increase in $Đ$ can be leveraged to control nanoparticle dispersion in complex media.

■ ASSOCIATED CONTENT

Supporting Information

The Supporting Information is available free of charge at https://pubs.acs.org/doi/10.1021/acsmacrolett.0c00898.

Synthetic procedures, brush and polymer characterization data, grafting density calculations, determination of r_c, υ, and the crossover value of $N_w\sigma^{1/2}$ in the CPB regime from brush data, calculation of σ of PCL brushes, quantification of scaling exponents, and tabulated brush properties provided in Schemes S1−S3, Figures S1−S6, and Tables S1−S3 (PDF)

■ AUTHOR INFORMATION

Corresponding Authors

Jacinta C. Conrad − *William A. Brookshire Department of Chemical and Biomolecular Engineering, University of Houston, Houston, Texas 77204, United States;* orcid.org/0000-0001-6084-4772; Email: jcconrad@uh.edu

Megan L. Robertson − *William A. Brookshire Department of Chemical and Biomolecular Engineering and Department of Chemistry, University of Houston, Houston, Texas 77204, United States;* orcid.org/0000-0002-2903-3733; Email: mlrobertson@uh.edu

Authors

Tzu-Han Li − *Materials Science and Engineering Program, University of Houston, Houston, Texas 77204, United States*

Vivek Yadav − *William A. Brookshire Department of Chemical and Biomolecular Engineering, University of Houston, Houston, Texas 77204, United States;* orcid.org/0000-0003-3630-2767

Complete contact information is available at: https://pubs.acs.org/10.1021/acsmacrolett.0c00898

Author Contributions

All authors have given approval to the final version of the manuscript.

Notes

The authors declare no competing financial interest.

■ ACKNOWLEDGMENTS

We thank Peter Vekilov and Mohammad Safari for access to and training on the dynamic light scattering instrument. We thank Scott Smith for access and training in the University of Houston Department of Chemistry Nuclear Magnetic Resonance Facility. We thank Jeffrey Rimer and Thuy Le for access to the HF fume hood and Ryan Poling-Skuvik, Tyler Cooksey, and Ali Slim for assisting with HF experiments. We thank Ramanan Krishnamoorti and Katrina Mongcopa for access to thermogravimetric analysis. Finally, we thank Katrina Mongcopa, Ryan Poling-Skutvik, and Wenyue Ding for helpful advice on SI-ATRP. We acknowledge support from the American Chemical Society Petroleum Research Fund (Grant 58531-ND7), the Welch Foundation (Grant E-1869), the National Science Foundation (Grants CBET-1437831 and DMR-1611376), and the University of Houston Grants to Enhance and Advance Research Program.

■ REFERENCES

(1) Choi, J.; Hui, C. M.; Pietrasik, J.; Dong, H.; Matyjaszewski, K.; Bockstaller, M. R. Toughening Fragile Matter: Mechanical Properties of Particle Solids Assembled from Polymer-Grafted Hybrid Particles Synthesized by ATRP. *Soft Matter* **2012**, *8* (15), 4072−4082.

(2) Jiao, Y.; Tibbits, A.; Gillman, A.; Hsiao, M.-S.; Buskohl, P.; Drummy, L. F.; Vaia, R. A. Deformation Behavior of Polystyrene-Grafted Nanoparticle Assemblies with Low Grafting Density. *Macromolecules* **2018**, *51* (18), 7257−7265.

(3) Kubiak, J. M.; Yan, J.; Pietrasik, J.; Matyjaszewski, K. Toughening PMMA with Fillers Containing Polymer Brushes Synthesized *via* Atom Transfer Radical Polymerization (ATRP). *Polymer* **2017**, *117*, 48−53.

(4) Bell, M.; Krentz, T.; Keith Nelson, J.; Schadler, L.; Wu, K.; Breneman, C.; Zhao, S.; Hillborg, H.; Benicewicz, B. Investigation of Dielectric Breakdown in Silica-Epoxy Nanocomposites Using Designed Interfaces. *J. Colloid Interface Sci.* **2017**, *495*, 130−139.

(5) Zorn, M.; Bae, W. K.; Kwak, J.; Lee, H.; Lee, C.; Zentel, R.; Char, K. Quantum Dot−Block Copolymer Hybrids with Improved Properties and Their Application to Quantum Dot Light-Emitting Devices. *ACS Nano* **2009**, *3* (5), 1063−1068.
(6) Grabowski, C. r. A.; Fillery, S. P.; Koerner, H.; Tchoul, M.; Drummy, L.; Beier, C. W.; Brutchey, R. L.; Durstock, M. F.; Vaia, R. A. Dielectric Performance of High Permitivity Nanocomposites: Impact of Polystyrene Grafting on BaTiO3 and TiO2. *Nanocomposites* **2016**, *2* (3), 117−124.
(7) Khabibullin, A.; Fullwood, E.; Kolbay, P.; Zharov, I. Reversible Assembly of Tunable Nanoporous Materials from "Hairy" Silica Nanoparticles. *ACS Appl. Mater. Interfaces* **2014**, *6* (19), 17306−17312.
(8) Zhi, S.-H.; Xu, J.; Deng, R.; Wan, L.-S.; Xu, Z.-K. Poly(vinylidene fluoride) Ultrafiltration Membranes Containing Hybrid Silica Nanoparticles: Preparation, Characterization and Performance. *Polymer* **2014**, *55* (6), 1333−1340.
(9) Qu, Z.; Xu, H.; Gu, H. Synthesis and Biomedical Applications of Poly((meth)acrylic acid) Brushes. *ACS Appl. Mater. Interfaces* **2015**, *7* (27), 14537−14551.
(10) Ballauff, M. Spherical Polyelectrolyte Brushes. *Prog. Polym. Sci.* **2007**, *32* (10), 1135−1151.
(11) Yuan, L.; Tang, Q.; Yang, D.; Zhang, J. Z.; Zhang, F.; Hu, J. Preparation of pH-Responsive Mesoporous Silica Nanoparticles and Their Application in Controlled Drug Delivery. *J. Phys. Chem. C* **2011**, *115* (20), 9926−9932.
(12) Giraud, L.; Bazin, G.; Giasson, S. Lubrication with Soft and Hard Two-Dimensional Colloidal Arrays. *Langmuir* **2017**, *33* (15), 3610−3623.
(13) Liu, G.; Cai, M.; Zhou, F.; Liu, W. Charged Polymer Brushes-Grafted Hollow Silica Nanoparticles as a Novel Promising Material for Simultaneous Joint Lubrication and Treatment. *J. Phys. Chem. B* **2014**, *118* (18), 4920−4931.
(14) Seymour, B. T.; Wright, R. A. E.; Parrott, A. C.; Gao, H.; Martini, A.; Qu, J.; Dai, S.; Zhao, B. Poly(alkyl methacrylate) Brush-Grafted Silica Nanoparticles as Oil Lubricant Additives: Effects of Alkyl Pendant Groups on Oil Dispersibility, Stability, and Lubrication Property. *ACS Appl. Mater. Interfaces* **2017**, *9* (29), 25038−25048.
(15) Yadav, V.; Hashmi, N.; Ding, W.; Li, T.-H.; Mahanthappa, M. K.; Conrad, J. C.; Robertson, M. L. Dispersity Control in Atom Transfer Radical Polymerizations Through Addition of Phenylhydrazine. *Polym. Chem.* **2018**, *9* (33), 4332−4342.
(16) Wang, J.-S.; Matyjaszewski, K. Controlled/"living" Radical Polymerization. Atom Transfer Radical Polymerization in the Presence of Transition-Metal Complexes. *J. Am. Chem. Soc.* **1995**, *117* (20), 5614−5615.
(17) von Werne, T.; Patten, T. E. Atom Transfer Radical Polymerization from Nanoparticles: A Tool for the Preparation of Well-Defined Hybrid Nanostructures and for Understanding the Chemistry of Controlled/"Living" Radical Polymerizations from Surfaces. *J. Am. Chem. Soc.* **2001**, *123* (31), 7497−7505.
(18) Pyun, J.; Matyjaszewski, K. Synthesis of Nanocomposite Organic/Inorganic Hybrid Materials Using Controlled/"Living" Radical Polymerization. *Chem. Mater.* **2001**, *13* (10), 3436−3448.
(19) Rungta, A.; Natarajan, B.; Neely, T.; Dukes, D.; Schadler, L. S.; Benicewicz, B. C. Grafting Bimodal Polymer Brushes on Nanoparticles Using Controlled Radical Polymerization. *Macromolecules* **2012**, *45* (23), 9303−9311.
(20) Ohno, K.; Morinaga, T.; Koh, K.; Tsujii, Y.; Fukuda, T. Synthesis of Monodisperse Silica Particles Coated with Well-Defined, High-Density Polymer Brushes by Surface-Initiated Atom Transfer Radical Polymerization. *Macromolecules* **2005**, *38* (6), 2137−2142.
(21) Matyjaszewski, K.; Dong, H.; Jakubowski, W.; Pietrasik, J.; Kusumo, A. Grafting from Surfaces for "Everyone": ARGET ATRP in the Presence of Air. *Langmuir* **2007**, *23* (8), 4528−4531.
(22) Martinez, A. P.; Carrillo, J.-M. Y.; Dobrynin, A. V.; Adamson, D. H. Distribution of Chains in Polymer Brushes Produced by a "Grafting From" Mechanism. *Macromolecules* **2016**, *49* (2), 547−553.
(23) Kruk, M.; Dufour, B.; Celer, E. B.; Kowalewski, T.; Jaroniec, M.; Matyjaszewski, K. Grafting Monodisperse Polymer Chains from Concave Surfaces of Ordered Mesoporous Silicas. *Macromolecules* **2008**, *41* (22), 8584−8591.
(24) Jiang, F.; Meyer, W. g. H.; Zhang, J. Dense poly(4-vinyl pyridine) Brushes Grafting from Silica Nanoparticles *via* Atom Transfer Radical Polymerization. *Colloids Surf., A* **2013**, *436*, 302−308.
(25) Savin, D. A.; Pyun, J.; Patterson, G. D.; Kowalewski, T.; Matyjaszewski, K. Synthesis and Characterization of Silica-Graft-Polystyrene Hybrid Nanoparticles: Effect of Constraint on the Glass-Transition Temperature of Spherical Polymer Brushes. *J. Polym. Sci., Part B: Polym. Phys.* **2002**, *40* (23), 2667−2676.
(26) Dukes, D.; Li, Y.; Lewis, S.; Benicewicz, B.; Schadler, L.; Kumar, S. K. Conformational Transitions of Spherical Polymer Brushes: Synthesis, Characterization, and Theory. *Macromolecules* **2010**, *43* (3), 1564−1570.
(27) Daoud, M.; Cotton, J. P. Star Shaped Polymers: a Model for the Conformation and its Concentration Dependence. *J. Phys. (Paris)* **1982**, *43* (3), 531−538.
(28) de Gennes, P. G. Conformations of Polymers Attached to an Interface. *Macromolecules* **1980**, *13* (5), 1069−1075.
(29) Lai, P. Y.; Halperin, A. Polymer Brush at High Coverage. *Macromolecules* **1991**, *24* (17), 4981−4982.
(30) Shim, D. F. K.; Cates, M. E. Finite Extensibility and Density Saturation Effects in the Polymer Brush. *J. Phys. (Paris)* **1989**, *50* (24), 3535−3551.
(31) Song, Y.; Yu, J.; Dai, D.; Song, L.; Jiang, N. Effect of Silica Particles Modified by *in-situ* and *ex-situ* Methods on the Reinforcement of Silicone Rubber. *Mater. Des.* **2014**, *64*, 687−693.
(32) Wijmans, C. M.; Zhulina, E. B. Polymer Brushes at Curved Surfaces. *Macromolecules* **1993**, *26* (26), 7214−7224.
(33) Karim, A.; Satija, S. K.; Douglas, J. F.; Ankner, J. F.; Fetters, L. J. Neutron Reflectivity Study of the Density Profile of a Model End-Grafted Polymer Brush: Influence of Solvent Quality. *Phys. Rev. Lett.* **1994**, *73* (25), 3407−3410.
(34) Lin, E. K.; Gast, A. P. Self Consistent Field Calculations of Interactions between Chains Tethered to Spherical Interfaces. *Macromolecules* **1996**, *29* (1), 390−397.
(35) Ohno, K.; Morinaga, T.; Takeno, S.; Tsujii, Y.; Fukuda, T. Suspensions of Silica Particles Grafted with Concentrated Polymer Brush: Effects of Graft Chain Length on Brush Layer Thickness and Colloidal Crystallization. *Macromolecules* **2007**, *40* (25), 9143−9150.
(36) Dodd, P. M.; Jayaraman, A. Monte Carlo Simulations of Polydisperse Polymers Grafted on Spherical Surfaces. *J. Polym. Sci., Part B: Polym. Phys.* **2012**, *50* (10), 694−705.
(37) de Vos, W. M.; Leermakers, F. A. M. Modeling the Structure of a Polydisperse Polymer Brush. *Polymer* **2009**, *50* (1), 305−316.
(38) Bentz, K. C.; Savin, D. A. Chain Dispersity Effects on Brush Properties of Surface-Grafted Polycaprolactone-Modified Silica Nanoparticles: Unique Scaling Behavior in the Concentrated Polymer Brush Regime. *Macromolecules* **2017**, *50* (14), 5565−5573.
(39) Petroff, M. G.; Garcia, E. A.; Dengler, R. A.; Herrera-Alonso, M.; Bevan, M. A. kT-Scale Interactions and Stability of Colloids with Adsorbed Zwitterionic and Ethylene Oxide Copolymers. *Macromolecules* **2018**, *51* (22), 9156−9164.
(40) Frisken, B. J. Revisiting the Method of Cumulants for the Analysis of Dynamic Light-Scattering Data. *Appl. Opt.* **2001**, *40* (24), 4087−4091.
(41) Aboudzadeh, M. A.; Iturrospe, A.; Arbe, A.; Grzelczak, M.; Barroso-Bujans, F. Cyclic Polyethylene Glycol as Nanoparticle Surface Ligand. *ACS Macro Lett.* **2020**, *9*, 1604−1610.
(42) Qi, S.; Klushin, L. I.; Skvortsov, A. M.; Schmid, F. Polydisperse Polymer Brushes: Internal Structure, Critical Behavior, and Interaction with Flow. *Macromolecules* **2016**, *49* (24), 9665−9683.
(43) Baker, J. A.; Pearson, R. A.; Berg, J. C. Influence of Particle Curvature on Polymer Adsorption Layer Thickness. *Langmuir* **1989**, *5* (2), 339−342.

https://doi.org/10.1021/acsmacrolett.0c00898
ACS Macro Lett. 2021, 10, 518−524

(44) Rubinstein, M.; Colby, R. H. *Polymer Physics*; Oxford University Press: Oxford, U.K., 2003.
(45) Ortiz, C.; Hadziioannou, G. Entropic Elasticity of Single Polymer Chains of Poly(methacrylic acid) Measured by Atomic Force Microscopy. *Macromolecules* **1999**, *32* (3), 780−787.
(46) Yamamoto, S.; Ejaz, M.; Tsujii, Y.; Fukuda, T. Surface Interaction Forces of Well-Defined, High-Density Polymer Brushes Studied by Atomic Force Microscopy. 2. Effect of Graft Density. *Macromolecules* **2000**, *33* (15), 5608−5612.
(47) Mendrek, B.; Trzebicka, B.; Wałach, W.; Dworak, A. Solution Behavior of 4-Arm Poly(*tert*-Butyl Acrylate) Star Polymers. *Eur. Polym. J.* **2010**, *46* (12), 2341−2351.
(48) Jehser, M.; Zifferer, G.; Likos, C. N. Scaling and Interactions of Linear and Ring Polymer Brushes *via* DPD Simulations. *Polymers* **2019**, *11* (3), 541.
(49) Hore, M. J. A. Polymers on Nanoparticles: Structure & Dynamics. *Soft Matter* **2019**, *15* (6), 1120−1134.
(50) Wei, Y.; Xu, Y.; Faraone, A.; Hore, M. J. A. Local Structure and Relaxation Dynamics in the Brush of Polymer-Grafted Silica Nanoparticles. *ACS Macro Lett.* **2018**, *7* (6), 699−704.
(51) Choi, J.; Hui, C. M.; Schmitt, M.; Pietrasik, J.; Margel, S.; Matyjazsewski, K.; Bockstaller, M. R. Effect of Polymer-Graft Modification on the Order Formation in Particle Assembly Structures. *Langmuir* **2013**, *29* (21), 6452−6459.
(52) Killgore, J. P.; Kocherlakota, L. S.; Overney, R. M. Enhanced Mobility and Increased Gas Sorption Capacity in Thin Film and Nanoconduit Confined Polymers. *J. Polym. Sci., Part B: Polym. Phys.* **2010**, *48* (4), 434−441.
(53) Cole, D. H.; Shull, K. R.; Baldo, P.; Rehn, L. Dynamic Properties of a Model Polymer/Metal Nanocomposite: Gold Particles in Poly(*tert*-butyl acrylate). *Macromolecules* **1999**, *32* (3), 771−779.

https://doi.org/10.1021/acsmacrolett.0c00898
ACS Macro Lett. 2021, 10, 518−524